

Supplemental material

Table of Contents

Supplementary Tables	2
Table 1. Clinical, histological features and percentage area of myeloperoxidase deposition in the renal biopsies of patients with various forms of CGN	2
Table 2. Correlation of intrarenal myeloperoxidase with clinical and histological parameters	3
Supplementary Figures.....	4
Figure 1. Purified human immunoglobulin-induced neutrophil degranulation.....	4
Figure 2. Inhibition studies of MPO by MPO-ANCA containing serum	5
Figure 3. Correlation of intrarenal MPO deposition with interstitial fibrosis and tubular atrophy and urinary protein: creatinine.....	6
Figure 4. Effect of AZM198 on PMA-induced NET formation.	7
Figure 5. Immunofluorescence staining for CD4 positive cells and neutrophils in the nephrotoxic nephritis model.	8
Figure 6. Pharmacokinetic studies of AZM198	9

Supplementary Tables

Table 1. Clinical, histological features and percentage area of myeloperoxidase deposition in the renal biopsies of patients with various forms of CGN

Diagnosis	eGFR at biopsy mls/min/1.73m ²	uPCR at biopsy mg/mmol	% Crescents	% IFTA	Total whole kidney MPO	Total tubulo- interstitial MPO	Total glomerular MPO	Extra- leukocyte glomerular MPO
MPA	35	240	30	50	2.66	5.31	10.37	4.4
GPA	46	235	85	30	2.25	9	10.8	4.6
MPA	37	228	50	40	2.02	9.5	13.5	2.5
MPA	28	274	70	20	3.66	12.3	12.9	5.9
GPA	13	737	85	50	3.042	5.7	14.5	6.9
ANCA negative	11	1747	40	40	4.674	7.8	13.16	6.3
ANCA negative	7	529	25	10	6.644	14	17.7	6.4
SLE	49	128	10	5	0.337	9	5.7	0.5
IgA	90	51	27	10	2.05	5	12.9	2.5
SLE	15	266	40	40	5.29	14	5.1	1.6
SLE	15	883	15	44	1.5	10.2	6.9	1.34
MPA	34	393	45	40	2.27	6.5	8.45	
MPA	88	10	5	5	0.2	2.1	3.6	
GPA	52	489	65	10	0.97	2	3.15	
IgA	14	416	30	5	0.82	2.4	3.2	
IgA	95	147	0	5	0.299	7.8	4	
IgA	90	150	12	5	0.897	7.5	5.9	
SLE	71	466	15	5	1.68	2.3	8.08	

Table 2. Correlation of intrarenal myeloperoxidase with clinical and histological parameters

		% crescents	% IFTA	eGFR at biopsy	uPCR at biopsy
Total MPO whole kidney	r	0.5822 ^c	0.6623 ^c	-0.6839 ^c	0.5067 ^c
	P value	0.0056	0.0014	0.0009	0.0159
Total tubulointerstitial MPO	r	0.1124	0.312	-0.4299 ^c	0.1168
	P value	0.3285	0.1037	0.0375	0.3222
Total glomerular MPO	r	0.424 ^c	0.532 ^c	-0.4525 ^c	0.2879
	P value	0.0398	0.0115	0.0297	0.1233
Extracellular glomerular MPO	r	0.6376 ^c	0.1871	-0.5845 ^c	0.492
	P value	0.0192	0.2885	0.0313	0.0632

^c Indicates a significant correlation

Supplementary Figures

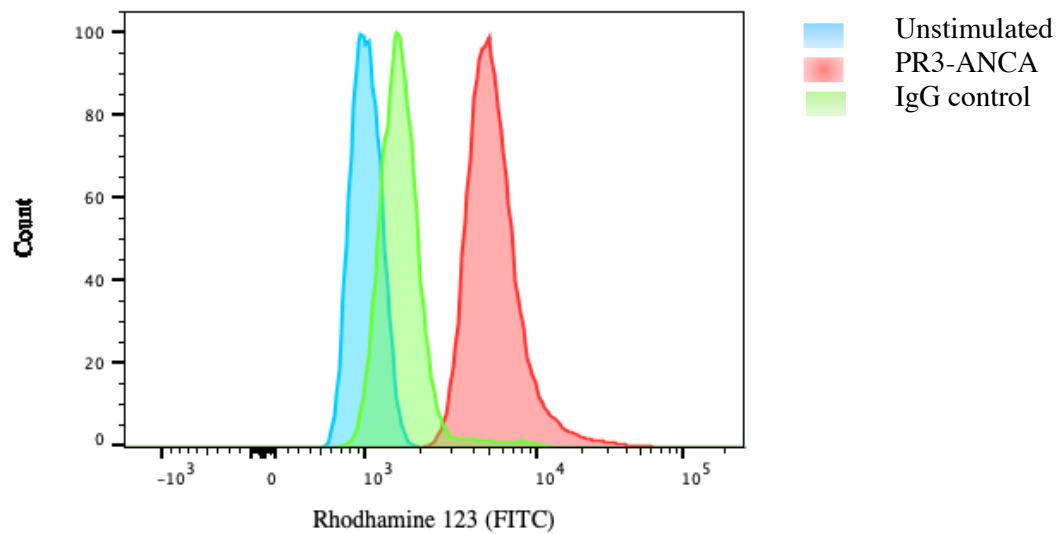


Figure 1. Purified human immunoglobulin-induced neutrophil degranulation

Histogram of rhodamine 123 (FITC) expression from unstimulated neutrophils or neutrophils stimulated with purified endotoxin-deplete PR3-ANCA or healthy control IgG (both used at $200\mu\text{g/mL}$) analysed by flow cytometry demonstrating ANCA-induced neutrophil degranulation

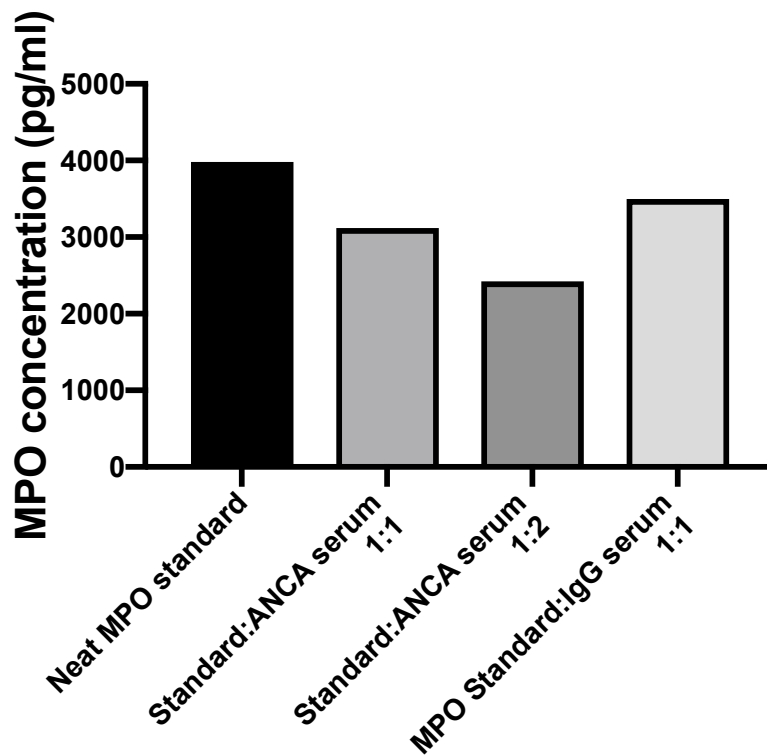


Figure 2. Inhibition studies of MPO by MPO-ANCA containing serum

Inhibition studies showing MPO concentration detected when human MPO standard (4000pg/mL) was incubated neat or after 1 hour incubation with MPO-ANCA containing serum in two dilutions and human IgG from a healthy control on pre-coated Elisa plates (MPO Elisa, DY3174).

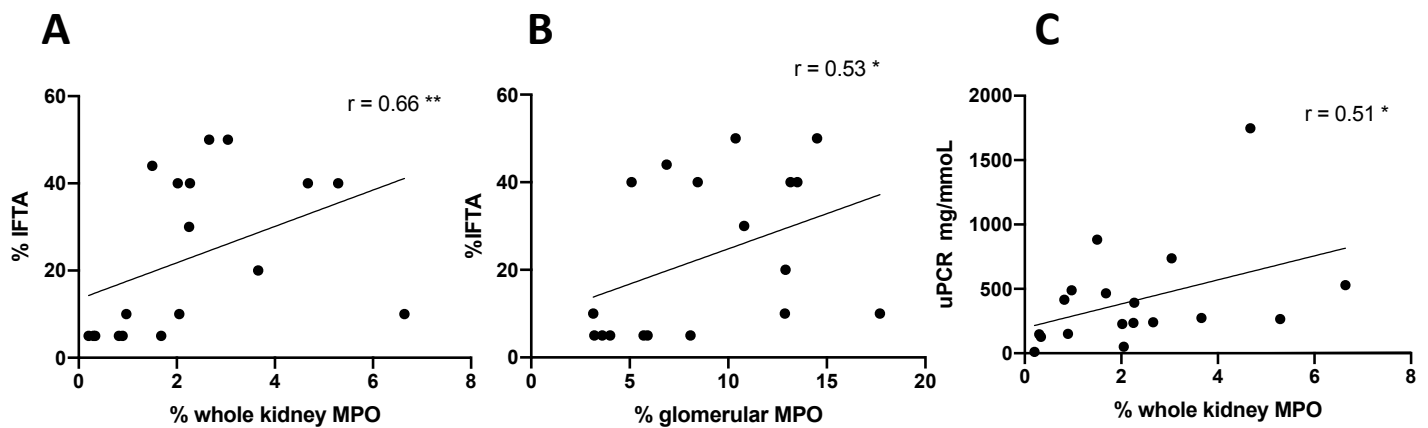


Figure 3. Correlation of intrarenal MPO deposition with interstitial fibrosis and tubular atrophy and urinary protein: creatinine.

Correlation between total whole kidney (A) or glomerular MPO deposition (B) (n=18) (percentage of myeloperoxidase stained area per whole kidney section or glomerulus) and interstitial fibrosis and tubular atrophy (IFTA) on renal biopsy, and C) between total whole kidney MPO and urinary protein: creatinine ratio (mg/mmol). Non-parametric Spearman rank correlation analysis, $^{*}P < 0.05$, $^{**}P < 0.01$. Biopsies from patients with diverse forms of CGN (MPO-ANCA=5, crescentic IgA=4, SLE =4, PR3-ANCA=3, ANCA negative =2).

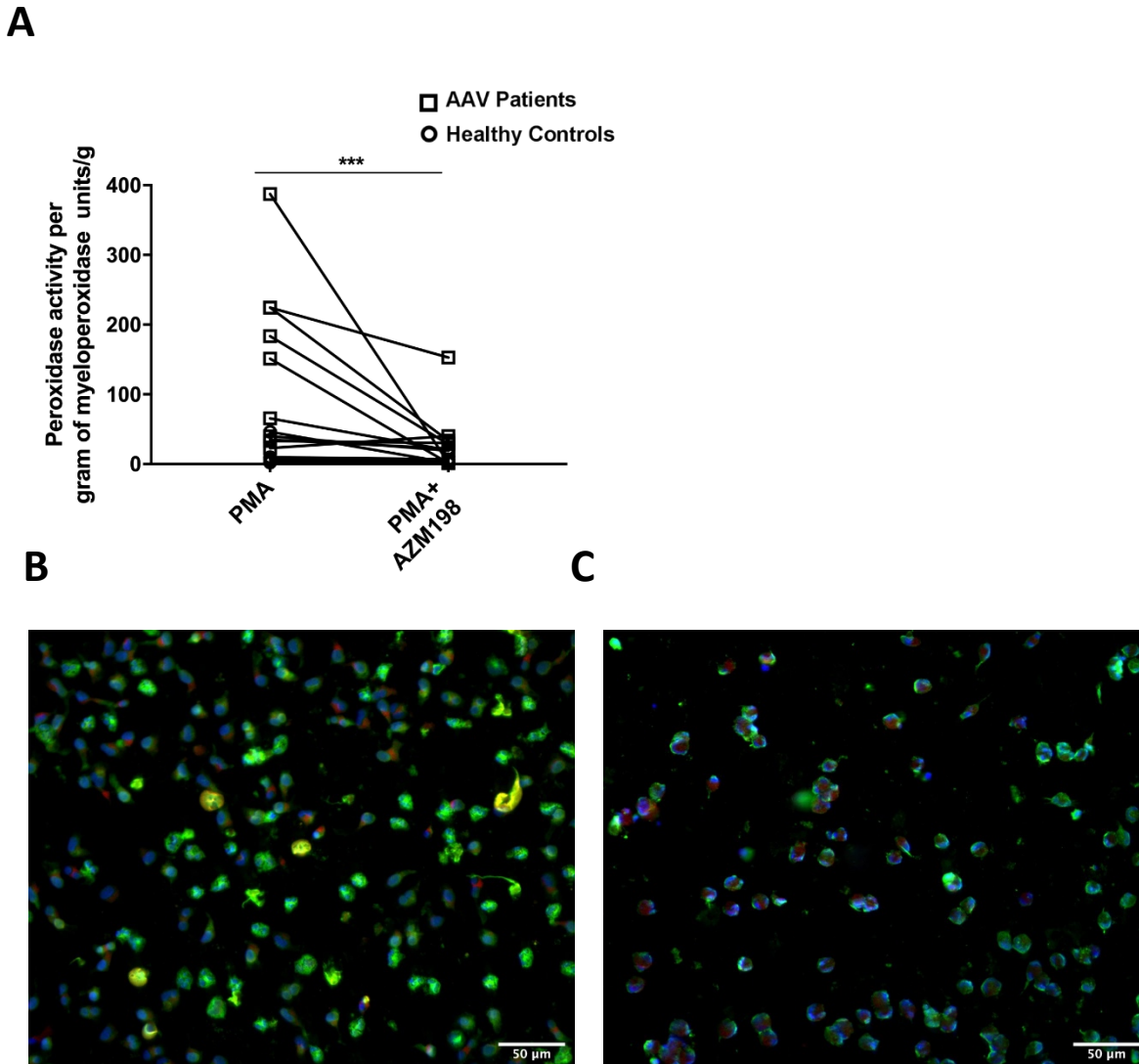


Figure 4. Effect of AZM198 on PMA-induced NET formation.

Effect of AZM198 on A) enzymatic myeloperoxidase activity (units/ g myeloperoxidase) in the supernatants of neutrophils from patients with AAV and healthy controls following 30 minute stimulation using PMA (n=16, 7 healthy controls, 6 MPO-ANCA, 3 PR3- ANCA), B) Merged microscopic images (x40 magnification) show NET formation and MPO (green)/elastase (red) colocalisation on NETs in the absence (B) or presence (C) of AZM198 (10 μ M) after 30min neutrophil stimulation with PMA from a patient with active MPO-ANCA disease.

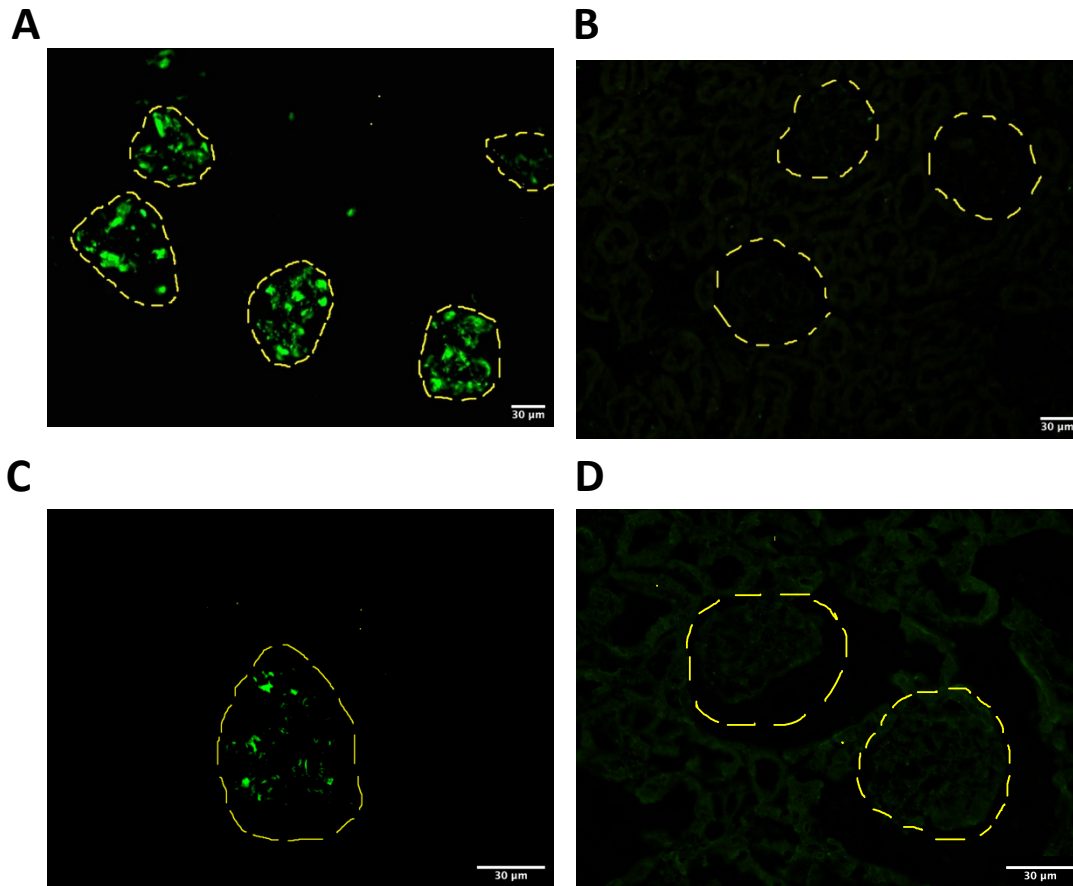


Figure 5. Immunofluorescence staining for CD4 positive cells and neutrophils in the nephrotoxic nephritis model.

Representative immunofluorescence staining for CD4 in the glomeruli of mice with NTN treated with A) vehicle or B) MPOi at 133μmol/kg and staining for neutrophils using Ly6g in mice dosed with either vehicle (C) or MPOi (D) twice a day at 133μmol/kg for 48 hours following the injection of nephrotoxic serum (NTS). Kidneys were collected 2 hours after NTS injection. Yellow lines outline glomeruli.

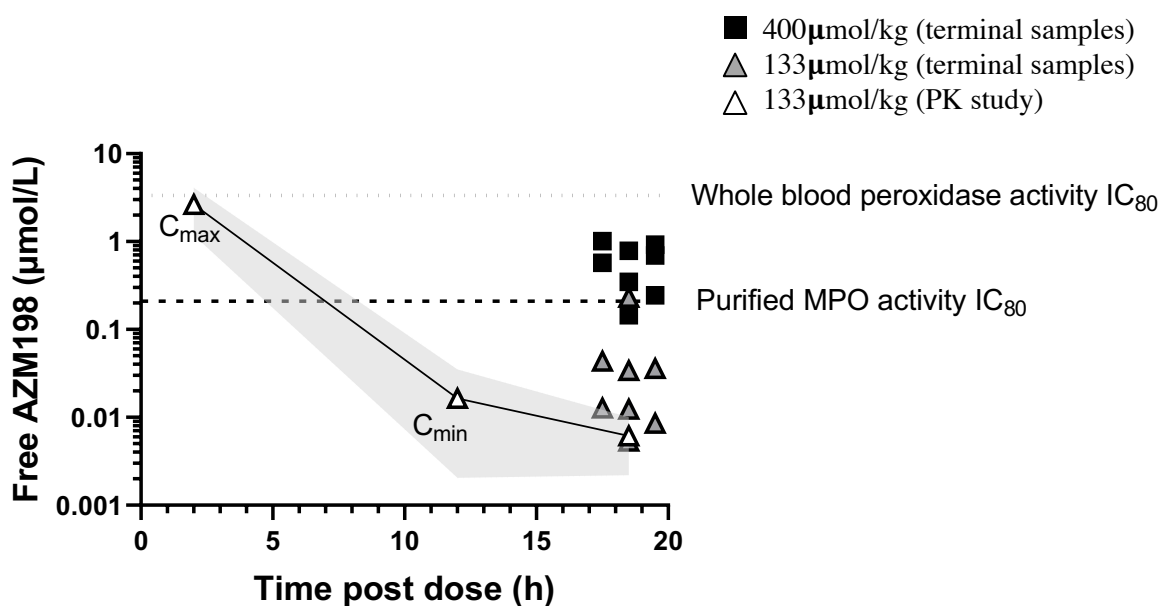


Figure 6. Pharmacokinetic studies of AZM198

Free plasma concentrations of AZM198. Mice were dosed every 12h with AZM198 and plasma concentration 19h after the final dose were measured (grey triangles represent the individual mice receiving 133 $\mu\text{mol/kg}$, and black squares 400 $\mu\text{mol/kg}$). A satellite group of mice were dosed with 133 $\mu\text{mol/kg}$ AZM198 and sampled at 2, 12 and 19h to measure the maximal (C_{max}) and trough (C_{min}) levels and to bridge the data to the terminal samples of the efficacy study, respectively ($n=3/\text{timepoint}$, white triangles represent mean values, grey area representing 95% confidence interval). The free plasma concentration of AZM198 corresponding to 80% inhibition of the activity of purified MPO is illustrated with a dashed line, and the concentration corresponding to 80% inhibition of peroxidase activity in zymosan-stimulated whole blood is illustrated with a dotted line.